Wind-Energy based Path Planning For Unmanned Aerial Vehicles Using Markov Decision Processes

Wesam H. Al-Sabban, Luis F. Gonzalez and Ryan N. Smith

***Abstract*— Exploiting wind-energy is one possible way to extend the flight duration of an Unmanned Aerial Vehicle. Wind-energy can also be used to minimise energy consumption for a planned path. In this paper, we consider uncertain, time-varying wind fields and plan a path through them that exploits the energy the field provides. A Gaussian distribution is used to determine uncertainty in the time-varying wind fields. We use a Markov Decision Process to plan a path based upon the uncertainty of the Gaussian distribution.**

Simulation results are presented to compare the direct line of flight between a start and target point with our planned path for energy consumption and time of travel. The result of our method is a robust path using the most visited cell while sampling the Gaussian distribution of the wind field in each cell.

I. INTRODUCTION

Small Unmanned Aerial Systems (UASs) have been widely developed for use in both military and civilian applications [1]. Such aircraft can be used for many applications such as coastal or border surveillance [2], atmospheric and climate research [3], as well as remote environment [4], forestry [4], agricultural [5], and oceanic monitoring [6] and imaging for the media and real-estate industries. However, one of the main limitations facing small UASs is their flight endurance with regard to the limitations of the possible on-board fuel/battery that can be carried [7]. Significant energy can be obtained from the environment if the energy sources can be exploited intelligently. Glider pilots and birds frequently use winds to increase range, endurance, or cross-country speed [8], [9].

There are three sources of wind energy available to exploit for this problem [10]:

1) Vertical air motion, such as thermal instabilities, orographic lift or wave.
2) Spatial wind gradients, such as horizontal shear layers.
3) Temporal gradients, causing horizontal gusts.

Although we can exploit all of these to some degree, difficulty arises due to the high variability in wind magnitude and direction. This is compounded by the difficulty to precisely forecast wind magnitude and direction and at multiple altitudes at different times. The magnitude and direction of the wind significantly affects the on-board power. Thus, optimal path planning considering variable and uncertain environmental conditions (horizontal wind, vertical wind) is a high importance for these vehicles to increase their efficiency by maximising flight duration and minimising power consumption. Converse to reducing power consumption, uncertain magnitude and direction of wind can actually cause uncontrollable forcing to be applied to the vehicle due to its small size [11]. This can have catastrophic effects. Figure 1 illustrates the concept of exploiting wind energy with a path from the starting point (Step 1) to a target point (Step 5) through a given wind field that is not a straight line.

The broad scope of this research is to develop an algorithm that can provide a time and energy efficient path by using the available environmental energy sources within the medium where the robot is operating while also considering the uncertainty of these sources. In this work, we proposed using an hybrid Gaussian distribution and a modified Markov Decision Processes (MDP) to identify the optimal path, minimum time-to-goal and minimum power consumption, for an UAS. The general MDP algorithm is based on dynamic programming; here we utilise value iteration [12] as our basis. Value iteration converges in polynomial time with respect to the number of iterations [13], [14]. We bound the number of cells and number of actions, and hence the number of iterations, based on the application domain and the assumed variability in the given wind field. However, we remark that the planning is assumed to be done offline, and not on-board the vehicle.

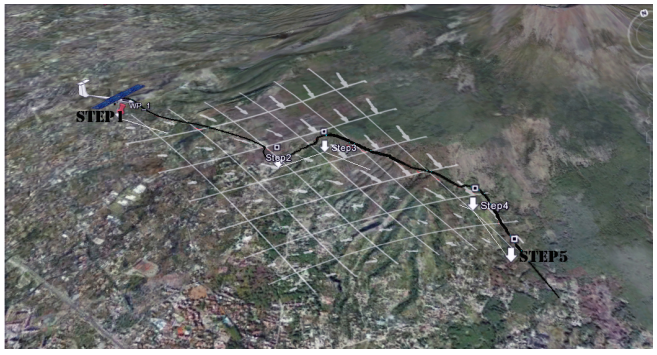

Fig. 1. A planned path that exploits wind energy from the start point (step1) to the target point (step5). While Step 2, Step 3 and Step 4 are the locations where the UAS changes the heading angle to follow the prescribed path.

II. RELATED WORK

The concept of extracting energy from the environmental forces has been applied in many different types of

W. Al-Sabban and L. Gonzalez are with the Australian Research Centre for Aerospace Automation, Queensland University of Technology, Brisbane, QLD, 4001 Australia. alsabban@student.qut.edu.au felipe.gonzalez@qut.edu.au

R.N. Smith is with the School of Electrical Engineering and Computer Science, Queensland University of Technology, Brisbane, QLD, 4001 Australia. ryan.smith@qut.edu.au

robots, such as UASs and Autonomous Underwater Vehicles (AUVs). Although we are primarily concerned with the aerial application in this study, the similarity of this problem to that of exploiting ocean currents with AUVs provides further motivation to accomplish our broader goal. Here, we introduce some relevant works in both the aerial and underwater domains, in which the authors utilised different techniques to exploit the available environmental energy in the medium of operation.

Langelaan [15], [16] for instance presented an approach to plan long distance trajectories for small UASs using orographic (i.e., slope) lift. The authors presented a tree-based approach, which uses a point mass model of the vehicle and knowledge of the wind field to generate feasible trajectories to a distant goal. Their work was limited to wind type and the change of the wind direction and magnitude with time and location. Chakrabarty and Langelaan [17] introduced a technique for long-range path planning for Small and Micro Unmanned Aerial Vehicles called Energy Maps, which calculates the minimum total energy needed to reach the target point, from a starting point while accounting for the effect of wind fields. This work does not consider the uncertainty of the wind field and the variation with respect to time. Chakrabarty and Langelaan [18] introduced an A* algorithm based on a cost function formed by the weighted sum of energy required and distance to goal. They compared the result of the required initial energy for varying weight with a wave-front expansion planning algorithm with the Energy Map approach introduced in [17]. In this work, the authors did not include variation of wind magnitude and direction with respect to time.

Researchers have also used probabilistic path planning to solve the problem of uncertainty in the wind magnitude and direction. Wolf, *et al.* [19] introduced a probabilistic motion planning algorithm in arbitrary, uncertain vector fields, with an emphasis on high-level planning for Montgolfiere balloons in the atmosphere of Saturn's Titan moon. The goal of the algorithm was to verify what altitude and horizontal actuation, if exist is available on the vehicle to apply to reach a goal point in the shortest expected time. In this work, the authors integrated the uncertainty of the wind field into the wind model and used a Markov Decision Process (MDP) for planning. The authors proposed that because the wind velocity is uncertain, the following horizontal position could be considered as a random variable, and a probability distribution can be built over all horizontally adjacent cells.Therefore, set these transition probabilities from all states the path planning problem become to select the actions (horizontal and vertical actuation of the balloon) that reduce time-to-goal. The MDP determines for every given current state, what is the optimal instant action so that the estimated cumulative time-to-goal is minimal. The authors applied the proposed technique on two cases: a stationary wind model, and a diurnally cyclical wind model.

Complementary to the research in UASs, a dual problem exists underwater and has been examined for AUVs. The path planning can be proposed very similarly with winds being exchanged with ocean currents. We include this literature as a complete survey of planning for vehicles moving in six degrees-of-freedom (DOF) and utilising environmental energy within the path planner. Garau, *et al.* [20] for example, used and adapted an A* algorithm to take current influence into account. The main disadvantages in their approach was that the variation of current with time was not addressed. Kruger, *et al.* [21] introduced a continuous approach to energy optimal path planning where time was considered as another search dimension which yield to optimise the vehicle thrust for minimal energy expenditure. The authors did not apply the optimisation techniques to find the globally optimal path in complex environments. In [22] Witt and Dunbabin built upon the work by Kruger [21], and proposed optimisation swarms to aid in finding paths that are close to the global-minimum. The examples considered in [21] involved a slightly simple artificial model of an estuary with stationary currents and obstacles, while in [22] the authors investigate more demanding planning cases in time-varying environments with dynamic obstacles using real ocean data. Rao and Williams [23] proposed a method for determining energy-optimal paths that account for the influence of ocean currents. The proposed technique was based on Rapidly-Exploring Random Trees (RRTs). The authors used data provided by ocean current forecasts. They also compared the result of RRT method to grid-based methods, and offered an improvement in terms of avoiding high-energy shallow regions.

In contrast to the aforementioned previous work, our proposed method offers the optimal energy-based path, the path that minimises the time-to-goal and the on-board energy usage, taking into consideration the variation of wind magnitude and direction with time to reach a specific target point through the novel combination of a Gaussian model and a modified MDP technique.

III. LATITUDINAL UAS DYNAMICS

We initially simplify the problem for this analysis by considering a planner problem in three DOF. This model will form a base for a path planner to be extended to six DOF. The three DOF are represented by $x-position, y-position$, and the heading angle ψ. The altitude of the UAS $z-position$ will remain constant for this study.

We define the variable W for the wind magnitude, Θ_W for wind direction, W_x for wind speed in the x direction, W_y for wind speed in the y direction, V_W as the UAS air speed and ψ for the heading angle. Additionally, let $\dot{X}_G$ and $\dot{Y}_G$ be the total velocity over ground in the x and y directions, respetively. Let $\dot{\psi}$ be the angular velocity of the UAS, V_w the UAS air speed, R_{min} the minimum turning radius, W_x and W_y are the wind speed in x and y directions respectively. Thus, X_G, Y_G and ψ represent the x-coordinate, y-coordinate, and heading angle, respectively, which identify the state of the UAS, and the corresponding equations of motion are then given by

$$\dot{X}_G = V_w \sin(\psi) + W_x, \tag{1}$$

$$\dot{Y}_G = V_w \cos(\psi) + W_y, \quad and \tag{2}$$

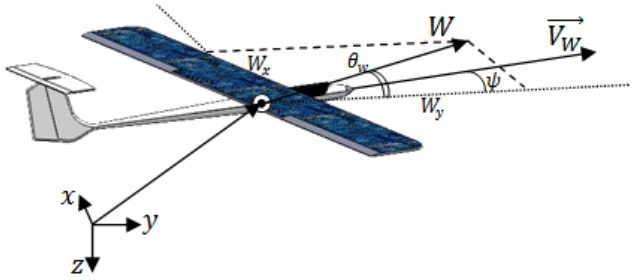

Fig. 2. Air-relative velocity and applied wind for a UAS. Here, W is the wind magnitude, Θ_W is wind direction, W_x wind speed in x direction, and W_y wind speed in y direction. V_W is the UAS air speed and ψ represents the heading angle.

$$\dot{\psi} = \frac{V_w}{R_{min}}\ U \quad (-1 < U < 1). \tag{3}$$

By integrating Eq. (3) with respect to time, we get

$$\psi = \psi_0 + \frac{V_w}{R_{min}}\ U\ t. \tag{4}$$

Substituting Eq. (4) into Eq. (1), we get

$$\dot{X}_G = V_w \sin(\psi_0 + \frac{V_w}{R_{min}}\ U\ t) + W_x, \quad and \tag{5}$$

$$\begin{aligned} \dot{X}_G \quad = \quad & V_w[(\cos(\frac{V_w}{R_{min}}\ U\ t)\sin(\psi_0)) \\ & +(\sin(\frac{V_w}{R_{min}}\ U\ t)\cos(\psi_0))U\ t) + W_x. \end{aligned} \tag{6}$$

By integrating Eq. (6), we get

$$X_G = \frac{-R_{min}}{U}\cos(\psi_0 + \frac{V_w}{R_{min}}\ U\ t) + W_x\ t\ + X_{G_0}. \tag{7}$$

Substituting Eq. (4) into Eq. (2), and by integrating the resultant equation, we get

$$Y_G = \frac{R_{min}}{U}\sin(\psi_0 + \frac{V_w}{R_{min}}\ U\ t) + W_y\ t\ + Y_{G_0}. \tag{8}$$

IV. PATH PLANNING

In this work, a Markov Decision Process (MDP) is used to find the optimal wind-energy based path for a UAS in the presence of a wind field distribution. The proposed path will provide the best path to follow to minimise the on-board electric power consumption of the UAS. The motion-planning problem is to select the actions that minimise the power consumption of the UAS and minimise time-to-goal. This problem is thus naturally posed as a Markov Decision Process $(S; A; P; R)$, where: S denotes the set of possible states of the aircraft; A is the set of actions available from each state; P presents the transition probabilities $P_a(s_i; s_j)$ where (s_i) is the current state and (s_j) is the possible next states under action (a); R defines the expected immediate reward for each transition and each action (a).

A. MDP Problem Description

Given two points (Start and Target) compute a path that minimises the time to goal by maximising the utility of an uncertain, time-varying wind field. The parameters of thi MDP problem are defined as follows.

Possible states (S): the number of possible states will be equal to the number of cells in the discretised grid. The Cartesian coordinates of the state of the UAS at the centre of a cell will be denoted by $S_{i,j} = x_{i,j}, y_{i,j}, \psi_{i,j}$ where $x_{i,j}, y_{i,j}, \psi_{i,j}$ denote x position, y position and heading angle for the UAS at cell$_{i,j}$ respectively. An important assumption is that the velocity of the aircraft is constant and equal to the Minimum Level-Flight Speed (V_{min}).

Actions available from each state (A): we assume that the UAS can move in eight directions, $A = N, NE, E, SE, S, SW, W, NW$ as shown in Fig. 3. where taking the action N means the heading angle (ψ) is equal to zero degree.

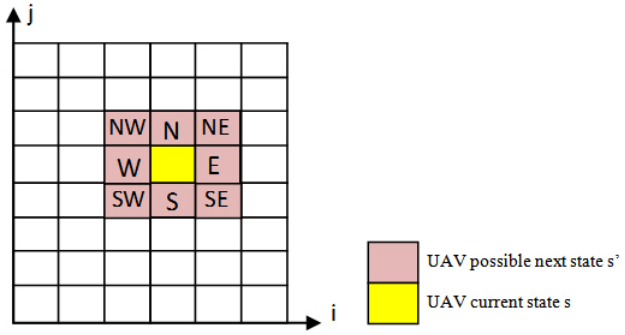

Fig. 3. A graphical representation of the eight possible end locations for the eight given actions of the UAS from a starting point in yellow and an ending state in pink.

Transition probabilities (P): the transition probabilities $P : P_{s,a}(s, \grave{s})$ manage the probabilities of what state $\grave{s}$ is entered after executing each action A from state s. In this work we develop a method based on Gaussian distribution to assign a realistic transition probabilities $P_{s,a}$ in time varying wind field to fit inside the MDP framework.

The time-varying wind field is approximated by a Gaussian distribution, at each time step a vector is chosen from the distribution to find the direction and magnitude of the wind field. In simulation, we consider both a uniform and non-uniform wind field. To determine the transition probabilities $P : P_{s,a}(s, \grave{s})$ the vector of the UAS velocity (V_{min}) with heading angle $(\psi_{i,j})$ and the chosen vector of wind velocity $(W_{i,j})$ with wind direction $(\theta_{i,j})$ at cell$_{i,j}$ are added. The summation result of the two vectors are represented by the magnitude $\overrightarrow{F}$ and direction ω using Eqs. (9)-(11).

$$F_x = V_{min}\cos(\psi_{i,j}) + W_{i,j}\cos(\theta_{i,j}), \tag{9}$$

$$F_y = V_{min}\sin(\psi_{i,j}) + W_{i,j}\sin(\theta_{i,j}), \quad and \tag{10}$$

$$\overrightarrow{F} = \sqrt{F_x^2 + F_y^2} \quad , \quad \omega = \tan^{-1}(\frac{F_y}{F_x}). \tag{11}$$

Figure 4 shows the normal distribution of transition probabilities (P) by setting ω from Eq. (11) as the mean value of a

Gaussian distribution with standard deviation σ in each cell. The standard deviation σ represents the average amount by which the heading angle in the distribution differ from the mean. The transition probabilities (P) will be represented by the area governed by the intersection between the curve and the range angle $\theta_a - \frac{\pi}{8}$ and $\theta_a + \frac{\pi}{8}$ (Green line) for each state Eq. (12). Here, the range angle provides the window for the possible next state for each action.

$$P : P_{s,a}(s, \grave{s}) = \frac{1}{\sigma\sqrt{2\pi}} \int_{\theta_a - \frac{\pi}{8}}^{\theta_a + \frac{\pi}{8}} e^{-\frac{1}{2}(\frac{v-\omega}{\sigma})^2} dv. \quad (12)$$

In this way, we differentiate our work from previous work by considering planning of a path over time-varying wind field using an MDP planner.

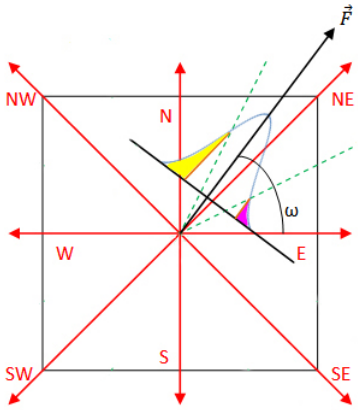

Fig. 4. The normal distribution of transition probabilities (P) by setting ω from Eq. (11) as the mean value of a Gaussian distribution with standard deviation σ_ω in each cell. In this example the total summation vector of the UAS velocity and wind velocity is represented by the black arrow, the probabilistic to reach the North state are shown by the yellow area, the probabilistic to reach the North-East state are shown by uncoloured area, the probabilistic to reach the East state are shown by the pink area.

Reward for each transition and each action (R): The direct reward value will be calculated based on the wind component facing the target cell Fig. 5. The ratio between the wind component facing the target point $(W_{i,j}\cos(\theta_{i,j} + \theta_T))$ and the maximum expected wind (W_{max}) value will be calculated and multiplying the result by a weight (C) - where (C) is selected by the user - using Eq. (13).

$$R_a(s_{i,j}) = (\frac{W_{i,j}\cos(\theta_{i,j} + \theta_T)}{W_{max}})C. \quad (13)$$

The value function $(V(s))$ for a cell will be equal to

$$V(s_{i,j}) := E[R_a(s_{i,j}) + \gamma \sum (P_{s,a}(s, \grave{s})V(\grave{s})]. \quad (14)$$

The optimal value function $(V^*(s))$ for a cell is given by

$$V(s_{i,j}) := max_a E[R_a(s_{i,j}) + \gamma \sum (P_{s,a}(s, \grave{s})V(\grave{s})], \quad (15)$$

where s is the initial state, $\grave{s}$ the next possible state, $R_a(s_{i,j})$ is the possible reward in state $s_{i,j}$ taken an action a, $P_{s,a}(s, \grave{s})$ is the probability of reaching $\grave{s}$ while applying action a in state $s_{i,j}$, and $V(\grave{s})$ is the value function for state $\grave{s}$.

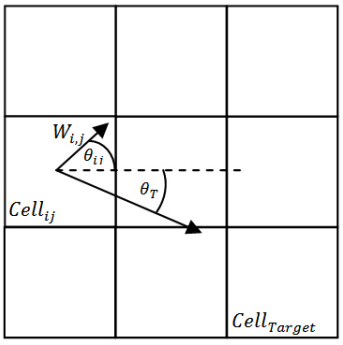

Fig. 5. Reward function. Where $(W_{i,j})$ is the wind magnitude at $(cell_{ij})$, (θ_{ij}) is the wind direction at $(cell_{ij})$ and (θ_T) is the direct angle between $(cell_{ij})$ and $(cell_{Target})$.

It is important to notice that applying Eq. (14) without using the discount factor γ may lead to the UAS not reaching the goal because the reward function is totally dependent on the harvested power. Thus the factor γ, representing the time ratio $(1 > \gamma > 0)$, is added to the equation.

Identifying the optimal values $V^*(s)$ will lead to determining the optimal policy $\pi^*(s)$ using

$$\pi^*(s) = arg\ max_a(R_a(s_{i,j}) + \gamma \sum_{\grave{s} \in S} P_{s,a}(s, \grave{s})V^*(\grave{s})). \quad (16)$$

Following this optimal policy will lead to computing the optimal path.

V. SIMULATIONS AND RESULTS

We applied the above approach to three cases considering a time-variant wind field which depends on Gaussian distribution as explained in Section IV-A. In the first presetned case, we will assume a constant wind field. The second case presented will change the wind direction in the middle of the grid to see the behaviour of the MDP path planner. The final case presented changes the value of the wind magnitudes and directions by $(\zeta\ \sigma_W)$ and $(\zeta\ \sigma_\theta)$, where $(-1 \geq \zeta \leq 1)$ and (σ_W) is the standard deviation of the wind magnitude and (σ_θ) is the standard deviation of the wind direction to find all possible paths.

A. MDP Path in Uniform Wind Flow

Case 1: We assume that the mean value of the wind speed and direction in each cell as a single vector which represents the wind (W) as shown in Fig. 6. We assume that the minimum velocity of the aircraft is $V_{min} = 20$ m/s, maximum possible wind $W_{max} = 15$ m/s , and constant weight factor $C = 30$.

Figure 7 shows the optimal path. It can be seen that the MDP method does not produce a straight line between the starting cell and the target cell. The reason is that the method uses the wind field and MDP to find the highest gain cell to reach the target by using the minimum on-board energy.

B. MDP Path in Nonuniform Wind Flow

Case 2: We assume that the mean value of the wind speed and direction in each cell as single vector which represents

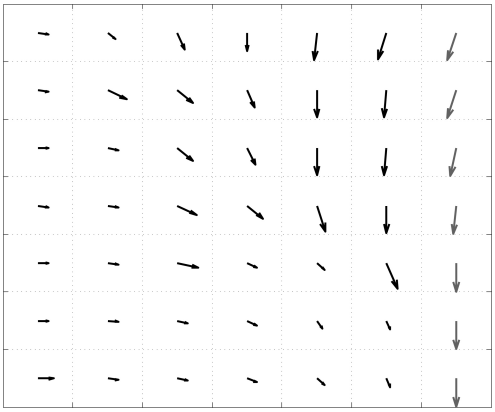

Fig. 6. Wind field distribution for Case 1, where the heads of arrows show the direction of the wind and the length of the arrows show the magnitude of the wind (5 - 15 m/s).

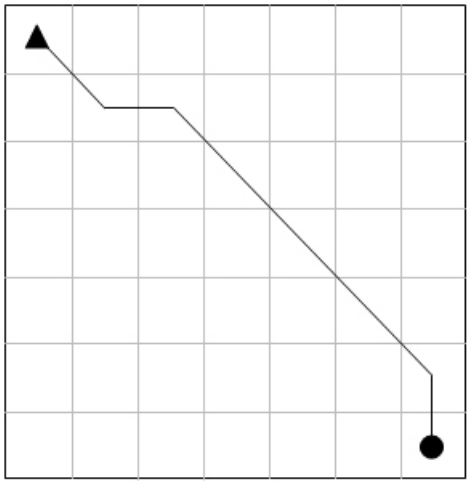

Fig. 7. MDP simulation result path for Case 1. The triangle is the starting point, and the circle is the target point.

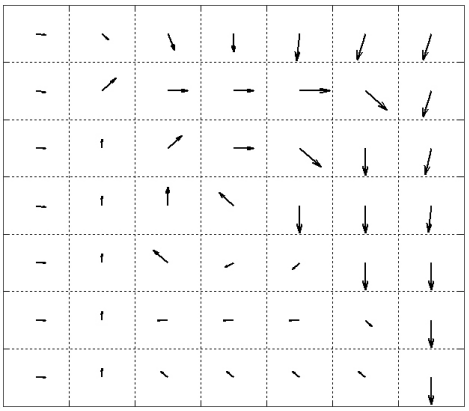

Fig. 8. Wind field distribution for case 2, where the head of arrows show the direction of the wind and the length of the arrows show the magnitude (5 - 15 m/s).

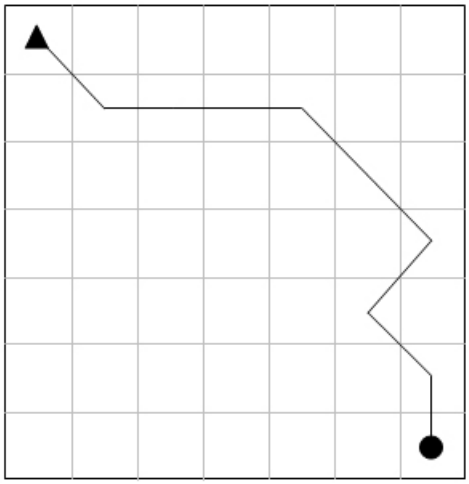

Fig. 9. Simulation resultant MDP path for Case 2, where the triangle is the starting point, and the circle is the target point.

the wind (W, θ) as shown in Fig. 8. The difference from the previous case is that we changed the wind direction in the middle of the grid. The reason to do this test is to validate the algorithm and demonstrate how it will avoid an unwanted wind field distribution which leads to high power consumption or/and high drift from the prescribed path.

It can be seen in Fig. 9 that the MDP planner avoided an unwanted wind and find its way to the goal. however, the trajectory jump to the left in cell (row=4, col=7) instead of following a straight line towards the target point. The reason for this is that we did not include the cost of a change in heading angle within the overall cost function.

C. MDP Path in Different Time-Varying Wind Fields

Since the value function of the cells is based on a probability distribution rather than a single scalar value, we can produce not only the most-likely wind-energy path between two points on the map, but also sample from the wind probability distribution to produce a distribution of paths between the two points. Results are shown in the form of planned paths between the starting point and target point over the grid, these paths are shown to vary in response to local variations in value function Fig. 10.

Case 3: We use the same wind field distribution provided in Case 1, however after finding the optimal path (which is the same as that shown in Case 1) the wind distribution is changed by (σ to $-\sigma$) with a 0.1 step increments. Then we compute the optimal path by choosing the most visited cell between the starting and the target cell to provide the optimal robust path because the probability of wind magnitude and direction at each cell in the grid contributes to identify the value function for each cell using MDP planner. This allows both the uncertainty in wind field and spatial variations in wind magnitude and direction to be incorporated into the planned path (red line) as shown in Fig. 10.

D. Discussion

As seen in the previous three cases, the algorithm successfully reached the target point in different wind field conditions. However, regarding the power consumption of the UAS, we want to know if this path is optimal. It is possible to compute the time required to reach the target point following

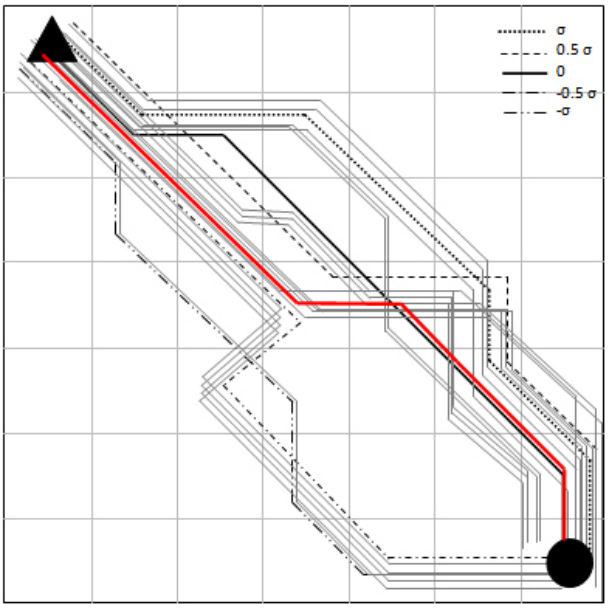

Fig. 10. Simulation resultant MDP path when the wind distribution is changed by (σ to $-\sigma$) with a 0.1 step increments. The red line is the most hit cell path.

the path generated by the algorithm and the direct straight line path between the starting and target points by taking into consideration the wind magnitude and direction in each cell and neglecting the possible drift of the aircraft caused by the wind. Assuming each cell is 1 km by 1 km, we apply the wind field distribution and using values shown in Case 2 Fig. 8. Figure 11 shows displacement versus time, with the dashed line represents our MDP path, and the solid line representing the straight line path.

As shown in Fig. 11, the MDP path has a longer distance to reach the target as compared with the straight line, however the time required to reach the target point using the MDP path is less than the time required using the straight line path. Since the throttle of the aircraft is constant for all three cases, the less time required to reach the goal, the less energy the aircraft will use to reach the goal. We can determine the efficiency of the MDP path as follows.

$$Eff_{path} = \frac{(T_{SL}) - (T_{MDP})}{(T_{SL})} \times 100, \qquad (17)$$

where (Eff_{path}) represents the efficiency of the path, (T_{SL}) represents the time required to reach the goal using a straight line, and (T_{MDP}) represents the time required to reach the goal using MDP method. The efficiency of the MDP resultant path for Case 2 is therefore,

$$Eff_{path} = \frac{(592.75) - (418.18)}{(592.75)} \times 100$$

$$Eff_{path} = 29.45\ \%$$

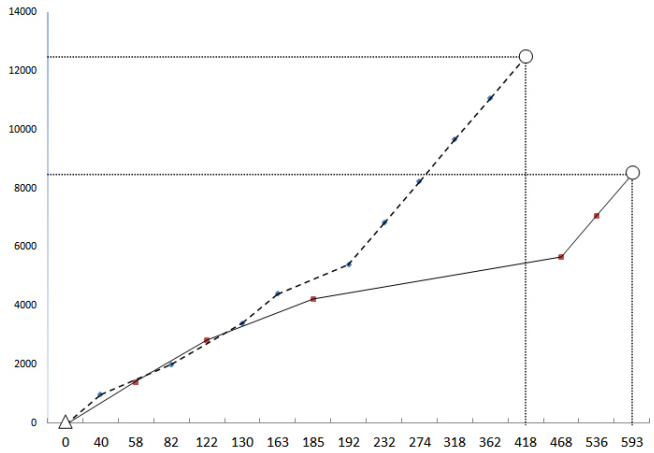

Fig. 11. Comparison between the time required to reach the target point using MDP path and straight line path between starting point and target point through wind field shown in Case 2. The plot is displacement versus time, with the dashed line representing the MDP path plot, and the solid line representing the straight line path.

VI. CONCLUSIONS

This paper presented a methodology for utilising an uncertain, time-varying wind field for a UAS using MDP. Simulated results demonstrate the validity of the planning for generating energy-paths in uncertain, time-varying wind fields. The use of a novel, hybrid Gaussian distribution of a wind field and the modified MDP technique with the velocity of the UAS to generate the probabilistic transition values provides not only an effective energy-path planning method which can effectively exploits the wind field, but also the robust path by using the most visited cells.

Future work will extend the current model and algorithm to six DOF and include the cost for a heading and other rotation angle changes. It is of interest to extend this study to plan missions for multiple vehicles, optimising for both coverage and time to goal for a team of vehicles. Additionally, we plan to apply the proposed algorithm on underwater vehicles to plan paths that exploit ocean currents for energy. Field trials for this work are planned for the middle part of 2013.

VII. ACKNOWLEDGEMENTS

R.N. Smith was supported in part by the Early Career Academic Recruitment and Development (ECARD) Program of the Queensland University of Technology.

REFERENCES

[1] J. Everaerts, "The use of unmanned aerial vehicles (uavs) for remote sensing and mapping," in *The International Archives of the Photogrammetry, Remote Sensing and Spatial Information Sciences*, vol. XXXVII, pp. 1187–1192, ISPRS Congress, 2008.

[2] R. B. Cathcart, C. W. Finkl, and V. Badescu, "Antarctica-to-western australia liquid freshwater shipments using stauber bags in a paternoster-like transfer system: Inaugurating a southern ocean antidrought action sea-lane," *Journal of Coastal Research*, pp. 1005–1018, Aug. 2011.

[3] H. Runge, W.Rack, A. Ruiz-Leon, and M. Hepperle, "A solar powered hale-uav for arctic research," in *preprint from the 1st CEAS European Air and Space Conference*, Sept. 2007, Berlin.

[4] W. AlSabban and L. Gonzalez, "Solar powered unmanned aerial vehicle: for fire prevention and planning," *in 2009 Design Challenge: Fire Research*, pp. 30–33, 2009.

[5] S. Herwitz, S. Dunagan, D. Sullivan, R. Higgins, L. Johnson, J. Zheng, R. Slye, J. Brass, J. Leung, B. Gallmeyer, and M. Aoyagi, "Solar-powered uav mission for agricultural decision support," in *Geoscience and Remote Sensing Symposium, 2003. IGARSS '03. Proceedings. 2003 IEEE International*, vol. 3, pp. 1692 – 1694, july 2003.

[6] A. Lomax, W. Corso, and J. Etro, "Employing unmanned aerial vehicles (uavs) as an element of the integrated ocean observing system," in *OCEANS, 2005. Proceedings of MTS/IEEE*, pp. 184 – 190 Vol. 1, 2005.

[7] A. J. Colozza, *Preliminary design of a long-endurance Mars aircraft*. NASA CR-185243, Washington, D.C.: National Aeronautics and Space Administration, 1990.

[8] M. J. Allen, "Updraft model for development of autonomous soaring uninhabited air vehicles," in *NASA Dryden Flight Research Center*, vol. 93523-0273, American Institute of Aeronautics and Astronautics, 2006.

[9] M. J. Allen and V. Lin, "Guidance and control of an autonomous soaring uav," Tech. Rep. NASATM2007214611, NASA Center for AeroSpace Information, 2007.

[10] J. W. Langelaan, "Biologically inspired flight techniques for small and micro unmanned aerial vehicles," in *Guidance, Navigation and Controls Conference*, vol. 2008-6511, American Institute of Aeronautics and Astronautics, 2008.

[11] J. Osborne and R. Rysdyk, "Waypoint guidance for small uavs in wind," *AIAA Infotech@ Aerospace*, pp. 1–12, 2005.

[12] R. Bellman, *Dynamic Programming*. Princeton University Press, 1957.

[13] B. Bonet, "On the speed of convergence of value iteration on stochastic shortest-path problems," *Mathematics of Operations Research*, vol. 32, no. 2, pp. 365–373, 2007.

[14] M. L. Littman, T. L. Dean, and L. P. Kaelbling, "On the complexity of solving markov decision problems," in *Proceedings of the Eleventh conference on Uncertainty in artificial intelligence*, UAI'95, (San Francisco, CA, USA), pp. 394–402, Morgan Kaufmann Publishers Inc., 1995.

[15] J. W. Langelaan, "Long distance/duration trajectory optimization for small uavs," in *Guidance, Navigation and Control Conference*, vol. 2007-6737, American Institute of Aeronautics and Astronautics, 2007.

[16] J. W. Langelaan, "Tree-based trajectory planning to exploit atmospheric energy," in *American Control Conference*, pp. 2328 – 2333, 2008.

[17] A. Chakrabarty and J. W. Langelaan, "Energy maps for long-range path planning for small- and micro - uavs," in *Guidance, Navigation and Control Conference*, vol. 2009-6113, American Institute of Aeronautics and Astronautics, 2009.

[18] A. Chakrabarty and J. W. Langelaan, "Flight path planning for uav atmospheric energy harvesting using heuristic search," in *Guidance, Navigation, and Control Conference*, vol. 2010-8033, American Institute of Aeronautics and Astronautics, 2010.

[19] M. T. Wolf, L. Blackmore, Y. Kuwata, N. Fathpour, A. Elfes, and C. Newman, "Probabilistic motion planning of balloons in strong, uncertain wind fields," in *IEEE International Conference on Robotics and Automation*, pp. 1123 – 1129, 2010.

[20] B. Garau, A. Alvarez, and G. Oliver, "Path planning of autonomous underwater vehicles in current fields with complex spatial variability: an a* approach," in *IEEE International Conference on Robotics and Automation*, pp. 194–198, 2005.

[21] D. Kruger, R. Stolkin, A. Blum, and J. Briganti, "Optimal auv path planning for extended missions in complex, fast-flowing estuarine environments," in *IEEE International Conference on Robotics and Automation*, pp. 4265 – 4270, 2007.

[22] J. Witt and M. Dunbabin, "Go with the flow: Optimal auv path planning in coastal environments," in *Australian Conference on Robotics and Automation*, 2008.

[23] D. Rao and S. B. Williams, "Large-scale path planning for underwater gliders in ocean currents," in *Australasian Conference on Robotics and Automation*, 2009.